THE JOURNAL OF PHYSICAL CHEMISTRY A
A JOURNAL OF THE AMERICAN CHEMICAL SOCIETY

pubs.acs.org/JPCA

Article

Coupled Cluster Benchmark of New DFT and Local Correlation Methods: Mechanisms of Hydroarylation and Oxidative Coupling Catalyzed by Ru(II, III) Chloride Carbonyls

Published as part of The Journal of Physical Chemistry virtual special issue "125 Years of The Journal of Physical Chemistry".

Irena Efremenko* and Jan M. L. Martin*

Cite This: *J. Phys. Chem. A* 2021, 125, 8987–8999

Read Online

ACCESS | Metrics & More | Article Recommendations | Supporting Information

ABSTRACT: We have evaluated a set of accurate canonical CCSD(T) energies for stationary points on the potential energy surface for Ru(II, III) chloride carbonyl catalysis of two competing reactions between benzene and methyl acrylate (MA), namely, hydroarylation and oxidative coupling. We have then applied this set to evaluate the performance of localized orbital coupled-cluster methods and several new and common density functionals. We find that (a) DLPNO-CCSD(T) with TightPNO cutoffs is an acceptable substitute for full canonical CCSD(T) calculations on this system; (b) for the closed-shell systems where it could be applied, LNO-CCSD(T) with tight convergence criteria is very close to the canonical results; (c) the recent ωB97X-V and ωB97M-V functionals exhibit superior performance to commonly used DFT functionals in both closed- and open-shell calculations; (d) the revDSD-PBEP86 revision of the DSD-PBEP86 double hybrid represents an improvement over the original, even though transition metals were not involved in its parametrization; and (e) DSD-SCAN and DOD-SCAN show comparable efficiency. Most tested (meta)-GGA and hybrid density functionals perform better for open-shell than for closed-shell complexes; this is not the case for the double hybrids considered.

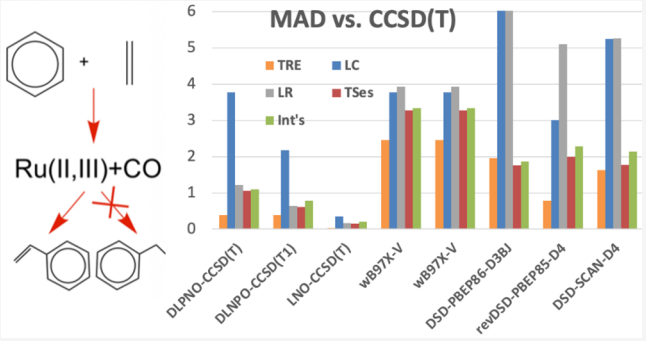

INTRODUCTION

Synthetic methods allowing one-step C−C bond formation through a metal-mediated transformation of C−H bonds have become increasingly important in both industry and basic research.[1−6] Potential routes for selective C−H bond activation and subsequent C−C bond formation in alkenes and aromatic compounds include the hydroarylation of unsaturated compounds by the addition of aromatic C−H bonds across an unsaturated C═C bond or their oxidative coupling that preserves the double bond. The latter reaction presents a highly desirable goal for industrial applications but is challenging from the synthetic point of view. Pioneering examples of Ru-catalyzed coupling of aromatic carbon−hydrogen bonds with olefins were reported two decades ago.[7−9] Since then, a growing number of coupling reactions catalyzed by Rh, Ru, and Pd have been published (e.g., reviews in refs 5 and 6), but the mechanistic aspects of the reactions are still not fully understood.

Motivated by the experimental results of Milstein and coworkers,[8] over a decade ago we first attempted to explore the mechanism of the oxidative coupling of arenes with alkenes in the presence of $[(\eta^6\text{-}C_6H_6)RuCl_2]_2$ or $RuCl_3{\cdot}3H_2O$ in a CO atmosphere as well as to compare it with the mechanism of the concurrent reaction of the hydroarylation of olefins (Scheme 1). In this preliminary work (reported in part in a conference proceedings extended abstract[10]), we employed hybrid and double-hybrid DFT.

In agreement with experiment, these calculations showed that under the reaction conditions both precatalysts transform to the respective Ru carbonyl chlorides. We found that the activation barriers, the relative energies of the key intermediates, and the overall direction of the catalytic reaction strongly depend on the composition of the Ru coordination sphere. Moreover, the energy results, particularly the calculated activation barriers, were hard to reconcile with experimental observations. In the present work, we have reexamined the mechanisms of Ru-catalyzed hydroarylation and oxidative coupling using wave

Received: June 10, 2021
Revised: September 15, 2021
Published: September 29, 2021

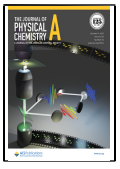

https://doi.org/10.1021/acs.jpca.1c05124
J. Phys. Chem. A 2021, 125, 8987−8999

Scheme 1. Interactions between MA and Benzene in the Presence of Ru(II, III) Chloride Carbonyl Complexes in Benzene Solution: Oxidative Coupling (Observed) and Hydroarylation (Not Observed)

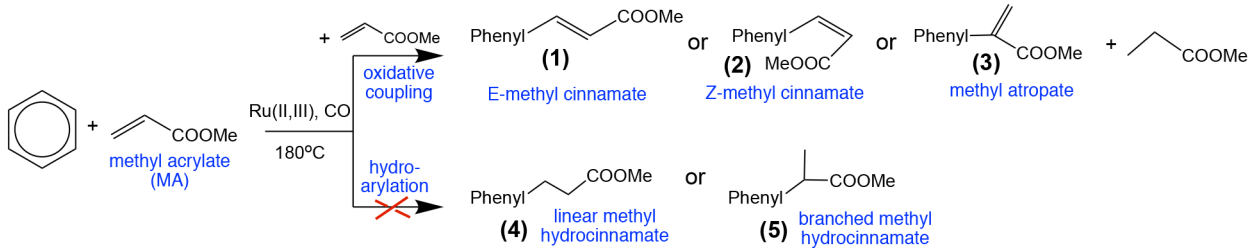

function theory (WFT) approaches up to and including canonical CCSD(T) (coupled cluster[11] with all single and double excitations[12] and a quasiperturbative correction for triple excitations[13,14]), which recently became feasible for real-size transition-metal systems. We have then used these latter results to assess the performance of more affordable computational methods.

The CCSD(T) method is considered to be the "gold standard" of quantum chemistry. However, the computational cost of canonical CCSD(T) calculations scales as $O(N^7)$ and becomes prohibitively high for mechanistic studies of practical transition-metal catalysis problems. Recently developed local correlation methods, such as DLPNO-CCSD(T) (domain localized pair natural orbital CCSD(T)) of Neese and co-workers,[15,16] PNO-LCCSD(T) (pair natural orbital, localized CCSD(T)) of Werner and co-workers,[17] and LNO-CCSD(T) of Nagy and Kállay,[18,19] scale almost linearly with system size in the large-molecule limit and, at least for main-group systems, provide similar accuracy to the corresponding canonical calculations (in addition to the original papers,[17,18] it has been shown by Neese and co-workers[20] and by our group[21]). For open-shell systems, several implementations aside from DLPNO-CCSD(T) have likewise been published, to wit: PNO-L methods,[22] LNO-CCSD(T)[23] (not yet available in MRCC[24] as of the time of writing), and the open-shell incremental methods of Dolg, Tew, and Friedrich.[25,26]

Recently, benchmark studies of the performance of density functionals for transition-metal problems, using DLPNO-CCSD(T) for calibration, have started appearing for reaction energies[27] and barrier heights.[28,29] Since the closed-shell Ru(II) and several open-shell Ru(III) complexes shown in Schemes 2 and 3 are still (barely) tractable by canonical methods on our available hardware, this enables us to assess the DLPNO error for real-size transition-metal complexes. In this article, we validate both WFT and DFT methods against canonical CCSD(T) for the hydroarylation and oxidative coupling of benzene and methyl acrylate (MA) catalyzed by $RuCl_2$ and $RuCl_3$ carbonyl complexes, as a representative example of the complex mechanisms of homogeneous catalytic reactions. Similar benchmark studies of commonly used density functionals in the prediction of thermochemistry and activation barriers of transition-metal-catalyzed reactions have been published. In some of these publications, the computational data are compared with experimental measurements.[30,31] In other publications, high-level coupled cluster calculations were used as a reference;[32−35] usually, such benchmark calculations were carried out for simplified model systems. The performance of the DLPNO-based coupled-cluster approach in closed- and open-shell systems has been tested for the very large and chemically diverse GMTKN55 (general main-group thermochemistry, kinetics, and noncovalent interactions, 55 problem sets) benchmark suite,[36] and it was shown that the iterative version[37,38] of the triples correction significantly reduced the discrepancy with canonical CCSD(T) for open-shell calculations.[20] (Concerning the proper use of DLPNO-CCSD(T), we also note recent work on nonheme iron complexes[39,40] and on spin crossover energetics.[41])

Keeping in mind specific computational problems usually addressed in such mechanistic studies, the calculations were divided into four groups: (i) overall reaction energies (Scheme 1) that do not involve transition metals; (ii) relative energies of stable $RuCl_n$ (n = 2, 3) complexes with CO, benzene, MA, and water (Schemes 2 and 3) that reproduce ligand coordination (**LC**) and ligand replacement (**LR**) reactions; (iii) energies of key intermediates along reaction pathways catalyzed by different Ru complexes (Scheme 4); and (iv) barrier heights along these reaction pathways.

COMPUTATIONAL METHODS

The Weigend−Ahlrichs basis set family[42] def2-TZVP, def2-TZVPP, and def2-QZVPP was used throughout because it was designed as a compromise between the requirements of wave function and DFT calculations. Reference geometries were optimized in the gas phase at the PBE0-D3BJ/def2-TZVP level[43−45] using Gaussian 16;[46] the identities of transition states were verified by frequency and intrinsic reaction coordinate calculations.

At the final geometries, canonical CCSD(T)/def2-TZVPP single-point energy calculations (without density fitting of any kind) were performed using MOLPRO,[47] both using default frozen cores and including the Ru(4s,4p) subvalence orbitals, which *are* correlated by default in ORCA ("chemical cores"). For closed-shell cases, RHF references were used; for open-shell cases, ROHF references were semicanonicalized and then used with the Watts−Gauss−Bartlett[14] definition of ROCCSD(T) (which, for etymological reasons, MOLPRO refers to as "rhf;uccsd(t)"). DLPNO-CCSD(T)[48] and the version with improved iterative triples, DLPNO-CCSD(T_1),[37] were calculated with the def-TZVPP basis set using ORCA[49] 4.1 and 4.2, as was DLPNO-CCSD(T)/def2-QZVPP; RIJCOSX was used here with program default grids and with the standard def2-TZVPP-RI[50,51] and def2-JK fitting basis[52] sets. The ECP is the standard Stuttgart ECP28MWB for Ru[53] associated with the def2 basis set family. (DLPNO-CCSD(T_1) for open-shell cases was first implemented in version 4.2. For want of an alternative, all open-shell DLPNO calculations were carried out using UHF references.) The DLPNO-CCSD(T)/def2-{T,Q}ZVPP results were extrapolated to the complete basis set limit using the simple L^{-3} formula,[54] which is functionally equivalent to the 2.970 extrapolation exponent found by Neese and Valeev.[55] Aside from the NormalPNO defaults, TightPNO cutoffs[56] were used to reduce domain discretization error. DLPNO-MP2,[57] RI-SCS-

https://doi.org/10.1021/acs.jpca.1c05124
J. Phys. Chem. A 2021, 125, 8987−8999

Scheme 2. Calculated $RuCl_2$ Complexes with Benzene, CO, and MA[a]

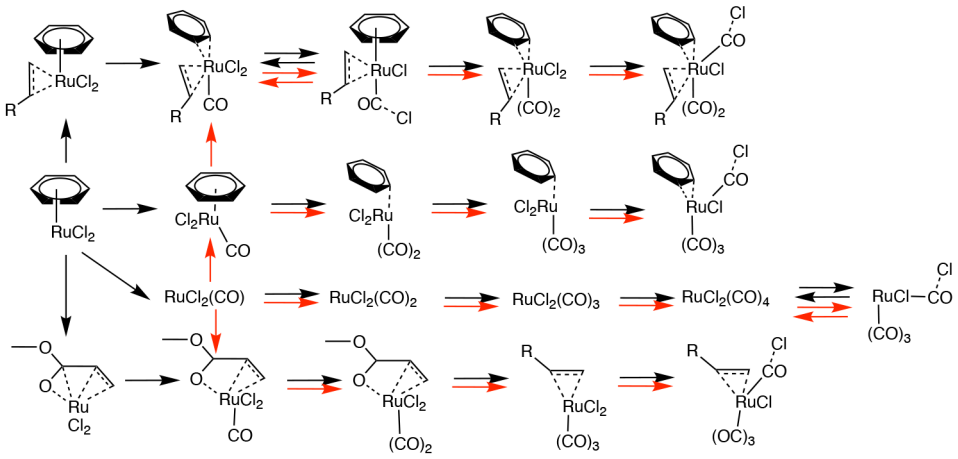

[a]Black arrows indicate the ligand replacement (**LR**) pathway with complex $[RuCl_2(C_6H_6)]$ used as a reference; red arrows show ligand coordination (**LC**) reactions with $RuCl_2(CO)$ used as a reference.

MP2,[58] and OO-RI-MP2[59,60] calculations in the def2-TZVPP basis set were likewise performed with ORCA default settings (and TightPNO for DLPNO-MP2).

In addition, single-point DFT calculations with a number of DFT functionals were carried out using ORCA. Aside from PBE0 as already mentioned, these include (a) the Berkeley "combinatorially optimized" B97M-V,[61] ωB97X-V,[62] and ωB97M-V;[63] (b) the M06 family:[64,65] M06-L, M06, and M06-2X; (c) TPSS[66] and two different hybrids thereof, namely,[66,67] TPSSh and TPSS0 (10 and 25% HF exchange, respectively); (d) density-corrected[68] HF-PBE0; (e) DOD-SCAN and DSD-SCAN with recently published[69] parameters; and (f) both the original double-hybrid DSD-PBEP86-D3BJ[70,71] and its reparametrized version revDSD-PBEP86-D4;[72] in the latter, D3BJ[44,73] was also replaced with the recently published next-generation D4 model.[74] Because the basis set convergence of double hybrids[75−78] tends to be dominated by the MP2-like term, we carried out def2-TZVPP and def2-QZVPP calculations and applied L^{-3} basis set extrapolation;[79] for the remaining DFT functionals, we applied def2-TZVPP except for ωB97{X,M}-V, which was accurate enough that we also tried def2-QZVPP followed by L^{-5} basis set extrapolation. GRID6 was used in all DFT calculations. In all ORCA calculations, both WFT and DFT, the RIJCOSX approximation[80,81] was applied (with ORCA4's default grid, GRIDXS2) along with the RI-MP2 approximation[82−86] for the double hybrids, both in conjunction with the respective appropriate density fitting and auxiliary basis sets[50,52,87,88] for the def2 family. For PBE0, SCAN, M06, TPSS, and double hybrid families, we checked the influence of Grimme's D3 and D4 dispersion corrections. The Becke−Johnson damping scheme that has the correct short-range behavior was combined with D3 for all of the functionals except for the M06 family, which already appears to cover intermediate-range dispersion,[89] and for which the original D3(0) scheme was used.

For another branch of double hybrids, namely, those based on the direct random phase approximation, we employed MRCC.[24] Specific functionals considered include the direct random phase approximation-based dual hybrid dRPA75[90] with a D3(0) dispersion correction[89] and its recently published spin-component-scaled variation SCS-dRPA75.[91] (The latter is equivalent to dRPA75 for closed-shell but not open-shell species. Only valence electrons were correlated in these calculations.) MRCC[24] was also used for the LNO-CCSD(T) approach of Nagy and Kállay,[18,19] where we used "normal" and "tight" screening criteria and additionally combined "tight" with `wpairtol=1e-6` following ref 92 (see below).

To check the influence of the lack of optimized atomic orbitals for subvalence correlation, additional canonical and LNO-CCSD(T) calculations were made using the cc-pwCVTZ-PP basis set for Ru.[93] For other elements, cc-PVTZ[94] and def2-TZVPP[42] basis sets were used in canonical and LNO-CCSD(T) calculations, respectively.

All molecules are neutral with the lowest multiplicity: singlet for closed-shell Ru(II) complexes and doublet for open-shell Ru(III) complexes. For open-shell DFT calculations in ORCA, UKS reference determinants were applied. Unless stated otherwise, all energy values presented in this article were obtained using the def2-TZVPP basis set with subvalence Ru 4s and 4p orbitals correlated in the reference canonical CCSD(T) calculations. Statistics with respect to our best CCSD(T) and DLPNO-CCSD(T1) basis set limit estimates can be found in the Supporting Information.

BENCHMARK DATABASE

Closed-Shell Ru(II) Complexes. Ru(II) complexes that may form in the reaction mixture and serve as the initial species of catalytic cycles are shown in Scheme 2. In most complexes, chloride anions are strongly bound to the metal atom; the exceptions are the highly coordinated complexes rightmost in each row of Scheme 2 and the $RuCl_2(CO)(MA)(C_6H_6)$ isomer with η^6 benzene coordination showing CO insertion into one of the Ru−Cl bonds. It would be natural to calculate the relative energies of the carbonyl complexes relative to $RuCl_2$, which is, however, a biradical in the ground state (*vide infra*). To avoid errors introduced by singlet−triplet separations represented by different methods, we considered two sets of reactions, ligand replacement (**LR**) and ligand coordination (**LC**). In the first set, indicated by black lines in Scheme 2, we used $RuCl_2(C_6H_6)$ as a reference because $RuCl_2$ will anyhow have no independent existence under the experimental conditions (benzene solvent). At all levels, the 1:1 exchange of benzene with CO or MA is energetically unfavorable; all other complexes are downhill relative to the reference. For the ligand coordination reactions

https://doi.org/10.1021/acs.jpca.1c05124
J. Phys. Chem. A 2021, 125, 8987−8999

outlined by red lines in Scheme 2, we excluded the three leftmost complexes and used $RuCl_2(CO)$ as the reference species. All in all, 24 **LR** and 20 **LC** reaction energies were calculated.

Open-Shell Ru(III) Complexes. In a similar manner, $RuCl_3(C_6H_6)$ was used as a reference for ligand replacement reactions in the open-shell Ru(III) complexes shown in Scheme 3 (black arrows) while ligand coordination energies were calculated relative to $RuCl_3$ (red arrows). Although this complex does not exist in the reaction mixture (water molecules in the coordination sphere of the initial form of catalyst $RuCl_3{\cdot}3H_2O$ are replaced by stronger-bonded benzene, MA, and CO ligands rather than dissociate), it is a natural reference species for the coordination of different ligands. Including all of the isomeric forms, 43 complexes were calculated. However, some of the complexes were too large for canonical CCSD(T) calculations, such that there were carried out only for 37 complexes (listed in Table S4) involved in 36 **LC** and **LR** reactions.

Scheme 3. Calculated $RuCl_3$ Complexes with Benzene, CO, H_2O, and MA[a]

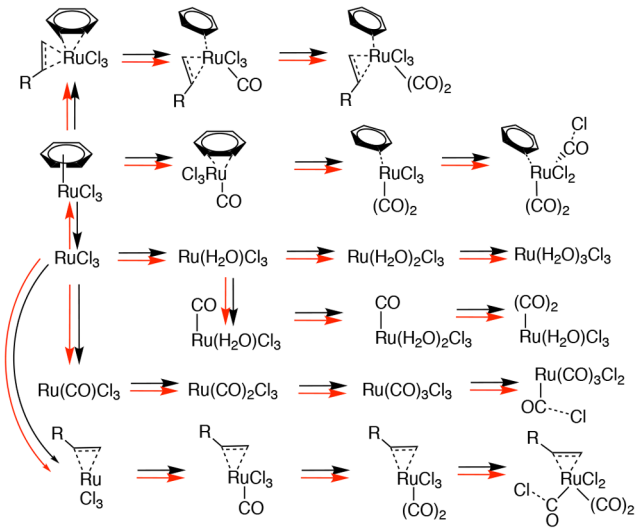

[a]Red arrows show ligand coordination (**LC**) reactions with $RuCl_3$ used as a reference; black arrows indicate ligand replacement reactions (**LR**) with $[RuCl_3(C_6H_6)]$ used as a reference.

Reaction Pathways. Our DFT calculations showed that in the presence of the Ru(II, III) complexes, either proton elimination by a chloride ion or hydrogen transfer from arene to a coordinated olefin can serve as an initial step in C−H bond activation, while other common mechanisms of C−H bond activation could be ruled out. Proton elimination proceeds via transition state **TS1** and leads to intermediate **Int1** with a reduced coordination number, according to Scheme 4a. Subsequent oxidative coupling with an olefin (**TS2**) leads to the formation of coordinated E-methyl cinnamate (**Int2**). The same intermediate can be obtained by initial MA activation (**MA-TS1**) followed by **MA-Int1** interaction with benzene via transition state **MA-TS2**. Consequent virtually barrierless methyl cinnamate dissociation and interaction of the resulting Ru hydride intermediate **Int3** with MA lead to fairly stable Ru alkyl complex **Int4**. The catalytic cycle could be closed by its interaction with benzene via transition state **TS3**, yielding **Int1**. Alternatively, **Int4** interaction with HCl (**TS4**) and benzene coordination regenerate the initial $RuCl_n(C_6H_6)$ carbonyl. Hydrogen transfer to MA (**TS1a** and **TS1b**) causes the coexistence of phenyl and one of the two isomeric alkyl ligands in the Ru coordination sphere (**Int1a** and **In1b**). This mainly leads to the hydroarylation products via **TS2a** and **TS2b** (Scheme 4b), but the coordination of the second olefin molecule followed by oxidative coupling is also possible in low-coordinated complexes.

For most intermediates and transition states, several isomers were calculated, such that the total numbers of calculated transition states and local minima on the closed-shell PES were 63 and 67, respectively; for the open-shell systems, 51 transition states and 50 intermediates were calculated. The relative energies of key intermediates and transition states along each reaction path were calculated relative to the initial form of the

Scheme 4. Mechanisms of MA Interactions with Benzene in the Presence of Ru(II, III) Chloride Carbonyl Complexes: Oxidative Coupling (a) and Hydroarylation (b)

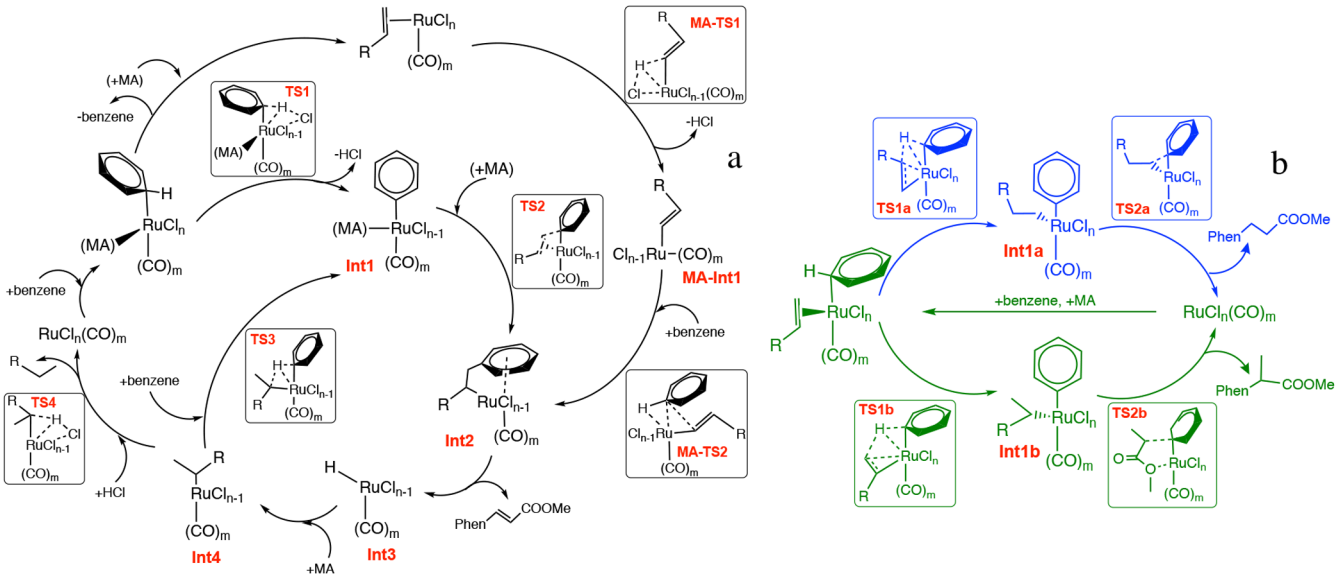

https://doi.org/10.1021/acs.jpca.1c05124
J. Phys. Chem. A 2021, 125, 8987−8999

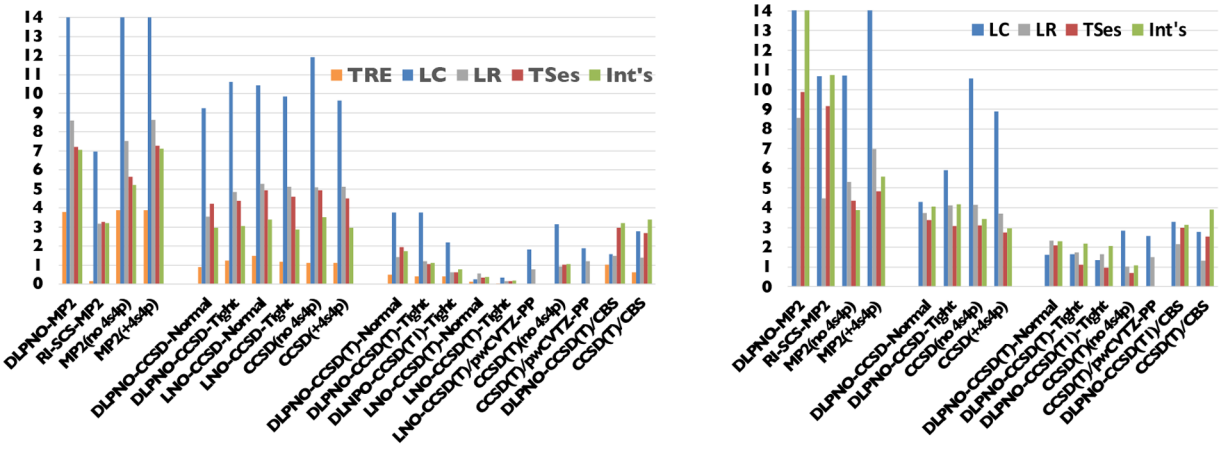

Figure 1. MAD relative to CCSD(T)/def2-TZVPP (kcal/mol) in canonical and DLPNO-based *ab initio* calculations for different types of energetics in the closed-shell (left) and open-shell (right) systems.

catalyst, the most stable isomer of $(C_6H_6)(CO)_nRuCl_2$ (n = 0−4) and $(C_6H_6)(CO)_nRuCl_3$ (n = 0−2). Several open-shell complexes are too large for canonical CC calculations; in this case, we used reduced data sets of 31 **TS**es and 25 intermediates listed in Tables S5−S6 compared to the canonical CC reference and full data sets with all of the calculated complexes and DLPNO-CCSD(T_1) energies used as a reference.

Optimized geometries of all of the complexes can be found in the Supporting Information (SI).

RESULTS AND DISCUSSION

Multireference Considerations. The close energy of transition-metal valence orbitals is a key feature in most of their practical applications, including catalysis. For this reason, transition-metal complexes often exhibit significant multireference character,[95−98] mostly type A static correlations[99] (a.k.a., absolute near-degeneracy correlation or left−right static correlation[100]). From a computational viewpoint, the usual single-reference techniques would no longer seem to be appropriate, yet some benchmark studies showed their applicability to transition-metal systems with mild to moderate static correlation.[101,102] There are several types of diagnostics for static correlation, which are briefly reviewed in ref 103. In the present work, we consider the simple T_1 diagnostic[104] and its matrix-norm counterpart, the D_1 diagnostic,[105] which are obtained as byproducts of our best canonical CCSD(T) calculations. For a subset of calculations performed with MOLPRO 2020 rather than earlier versions, the D_2 diagnostic[106] is also obtained. These diagnostics, together with the largest singles and doubles amplitudes, are collected in Tables S1−S6 of the SI. They are not foolproof by themselves and *a fortiori* do not characterize the nature of static correlation, but they do allow for qualitative insight into the nature of the wave function.[107]

Most of the closed-shell complexes have D_1 diagnostic values smaller than 0.2. The T_1 diagnostic values falling in the range of 0.02−0.03 indicate some multireference character but are smaller than the critical value of 0.045 proffered by Wilson and co-workers[98] for 4d transition-metal complexes.

One exception was singlet $RuCl_2$ with pathological D_1 and T_1 diagnostic values of 1.26 and 0.23, respectively, because the singlet is essentially purely low-spin biradical and biconfigurational: the ground state is a triplet. Another exception, the **TS2-CO2** complex, has a borderline T_1 = 0.05 but a pathologically large D_1 = 0.42: inspection of the cluster amplitudes reveals several prominent single excitations with amplitudes of up to 0.40. The **TS2-CO2** complex is too large for open-shell canonical CCSD(T) calculations; the DLPNO coupled-cluster calculations yielded CCSD energies of the singlet and triplet states within 1 kcal/mol, while the triples correction renders the triplet state 5.11 and 5.98 kcal/mol less stable than the singlet at the DLPNO-CCSD(T) and DLPNO-CCSD(T_1) levels, respectively. Test EOM-CCSD[108,109] calculations predict a first excitation energy of 33.0 kcal/mol. For several closed-shell complexes with D_1 > 0.14, we performed BCCD(T)/def2-SVP test calculations aimed to completely eliminate the single excitations (Table S7). These result in minor (less than 1 kcal/mol) increases in complexation energies for complexes with D_1 < 0.2. For the **TS2-CO2** case with its pathological (0.42) D_1 value, the BCCD(T) total energies is no less than 4 kcal/mol below their CCSD(T) counterparts. Another sign of significant static correlation is a sizable (T) contribution to the reaction energy of interest. It reaches 8.0 and 14.7 kcal/mol for several **LC** reactions and **TS**es, respectively. The decomposition of CCSD(T)/def2-TZVPP energies for several representative cases is shown in Tables S8 and S9. In the most troublesome cases, the triples correction makes a *positive* (i.e., antibonding) contribution to the energy of the complex. Thus, the formation of the **TS1-CO1-1** complex had a (T) contribution of 6.58 kcal/mol. In spite of reasonable D_1 and T_1 values (0.27 and 0.04, respectively), this complex showed exceptionally large deviations from the canonical CCSD(T)/def-TZVPP results, especially in MP2 calculations (surprisingly, in canonical and DLPNO with TightPNO but not with NormalPNO; LNO-CCSD(T) did not converge for this complex) and for extrapolation to CBS (up to 24 kcal/mol in CCSD(T)/CBS_{W1}). All three aforementioned complexes $RuCl_2$, **TS1-CO1-1**, and **TS2-CO2** are excluded from the statistics presented in this work. Several **Int3** intermediates that pose Ru−H bonding also had positive (T) contributions (particularly **Int3-CO1**, which has an RHF → UHF instability and an EOM-CCSD first excitation energy of 36.1 kcal/mol) but smaller D_1 (≤0.112) and T_1 (≤0.032) values. They did not show such exceptional behavior and thus were not excluded from the statistics.

For open-shell complexes, the D_1 and T_1 diagnostic values are slightly larger, up to 0.25 and 0.04, respectively. However, several complexes (**TS1-CO3**, **Int2**, and **Int4**) exhibit D_1 values of 0.38−0.42 and T_1 values of 0.044−0.055. The (T)

https://doi.org/10.1021/acs.jpca.1c05124
J. Phys. Chem. A 2021, 125, 8987−8999

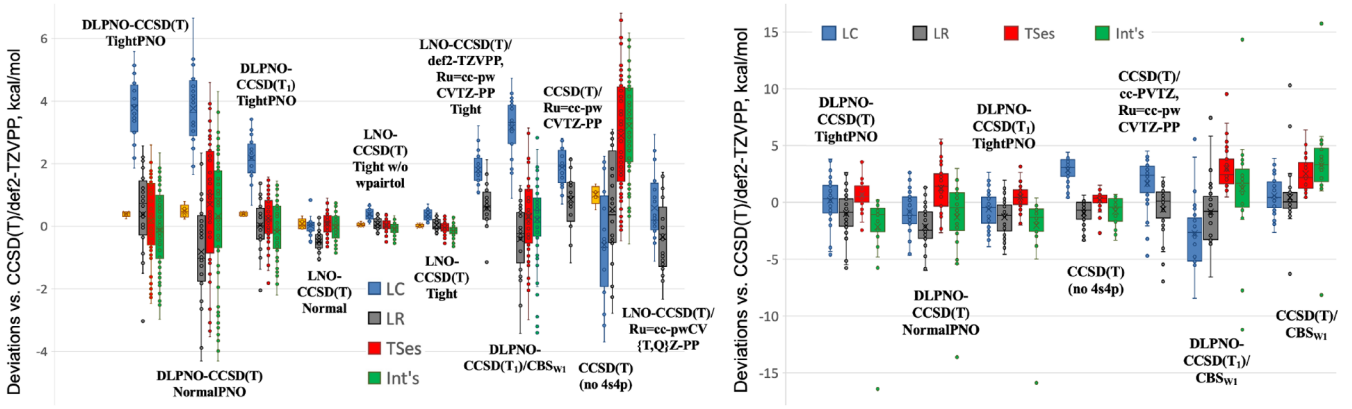

Figure 2. Statistical deviation of canonical and local correlation methods relative to canonical CCSD(T)/def2-TZVPP (kcal/mol) depending on the local orbitals' cutoffs and basis sets for different types of energetics in the closed-shell (left) and open-shell (right) systems.

contribution to the **LC** and **TSes** energies reaches 8.0 and 16.8 kcal/mol in several cases (Tables S8 and S9). Nevertheless, these complexes did not show exceptional deviations between localized and canonical coupled cluster and thus were not excluded from our statistical data sets. Although not exhaustive, this analysis indicates that wave functions of most Ru(II, III) complexes have mild to moderate multireference character; therefore, the CCSD(T) method should provide reasonably reliable reference energies for the present benchmark study in both closed- and open-shell cases.

Post-HF Canonical and Local Correlation Calculations. The MADs (mean absolute deviations) from canonical CCSD(T)/def2-TZVPP for five types of closed-shell and four types of open-shell energy differences are presented in Figure 1 and in Table S10 for various canonical and local correlation wave function levels of theory. Unless stated otherwise, the def2-TZVPP basis set was used throughout. The corresponding RMSD (root-mean-square deviation) and MSE (mean signed error) statistics as well as analogous data calculated relative to our CCSD(T) and DLPNO-CCSD(T1) basis set limit estimates can be found in Figures S1−S3 in the SI; corresponding numerical information (including maximum absolute deviations) can be found in Tables S11−S13. Canonical CCSD performed well for total reaction energetics (MAD = 1.1 kcal/mol); for intermediates and for open-shell **TSes**, the MAD is within 3 kcal/mol of the CCSD(T) results. The difference reaches 4.5 kcal/mol for Ru(II) **TSes**. The triples correction is critically important for ligand coordination: MAD reaches 9.64 and 8.90 kcal/mol for open- and closed-shell complexes, respectively, while ligand replacement is less sensitive, with MAD values of 5.11 and 3.69 kcal/mol. The DLPNO-CCSD results are usually very close to the canonical values, with differences in statistical deviations of 1.2 kcal/mol or less. The only exception is **LC** in open-shell complexes, for which the DLPNO-CCSD approach fortuitously "outperforms" canonical CCSD (MAD = 5.90 with TightPNO and 4.29 with NormalPNO vs 8.90 kcal/mol) due to error compensation. Comparing DLPNO-CCSD with canonical CCSD shows a strong dependence on the cutoffs: in closed-shell systems, MAD is less than 1 kcal/mol with TightPNO but reaches 2.46 and 1.36 kcal/mol for **LR** and **TSes** with NormalPNO. Similarly, in open-shell calculations, the deviation between canonical and DLPNO-based CCSD is almost halved for TightPNO compared to NormalPNO (3.97 vs 5.84, 1.13 vs 2.36, 0.70 vs 1.80, and 1.36 vs 2.19 for **LC**, **LR**, **TSes**, and **Int's**, respectively). The LNO-CCSD approach more closely tracks the canonical CCSD results, with the largest MAD of 0.79 kcal/mol found for **LC** with normal cutoffs. This latter value drops to 0.22 kcal/mol for LNO-CCSD Tight, with MADs for **LR**, **TS**, and **Int** not exceeding 0.14 kcal/mol.

The DLPNO-CCSD(T) TightPNO approach exhibits quite good agreement with the canonical results (MAD within 2.2 kcal/mol in all cases except for closed-shell **LC**, for which MAD = 3.77 kcal/mol). At least some of the remaining discrepancy appears to be due to the neglect of off-diagonal Fock matrix elements for the triples in the DLPNO-CCSD(T) approach: using the costlier DLNPO-CCSD(T_1) approach which does not make this approximation, MAD for ligand coordination in closed-shell complexes decreased by 1.59 kcal/mol while the energetics of other closed-shell reactions were improved by 0.3−0.6 kcal/mol. For open-shell energy differences, the influence was negligible (less than 0.3 kcal/mol). Extrapolation to the CCSD(T)/CBS_{W1} limit reveals an MAD (read, in this case, as the basis set incompleteness error) of up to 3.4 kcal/mol in the closed-shell calculations and up to 3.9 kcal/mol in the open-shell systems. The DLNPO-CCSD(T_1)/CBS_{W1} approach shows very close agreement (MAD = 0.39 kcal/mol) with canonical CCSD(T)/CBS_{W1} for the reaction energies, while for other groups of closed-shell calculations there is a bit more daylight between them (MAD = 2.18 for ligand coordination, 0.63 for **LR**, 0.61 for **TSes**, and 0.78 kcal/mol for **Int's**). The Ru(III) complexes showed even larger deviations (1.34, 1.64, 0.96, and 3.69, respectively).

For a normal distribution without systematic error, the RMSD/MAD ratio was shown by Geary[110] to be $(\pi/2)^{1/2}$ = 1.2533... ≈ 5/4. At the outlier DLNPO-CCSD(T_1) level, the RMSD/MAD ratios are close to that for Ru(II) **LC**, **LR**, and intermediates (1.05, 1.28, and 1.23) but much larger for **TSes** (1.79), indicating an outlier: we note that **TS2-CO2** is essentially biradical (and has D_1 > 0.4). If we exclude it, then MAD and RMSD drop to quite pleasing values of 0.61 and 0.73 kcal/mol, respectively, with the RMSD/MAD ratio being 1.20. The RMSD/MAD ratios for open-shell **LC**, **LR**, and **TSes** are close to the idealized values (1.23, 1.22, and 1.28) but much larger for intermediates (1.76); however, exclusion of the three complexes with D_1 values larger than 0.35 had only a minor influence on the statistics.

As for DLPNO-CCSD(T) NormalPNO (the ORCA default), the differences with DLPNO-CCSD(T_1) approach 2 kcal/mol, which enters the realm of the best DFT approaches (see below).

https://doi.org/10.1021/acs.jpca.1c05124
J. Phys. Chem. A 2021, 125, 8987−8999

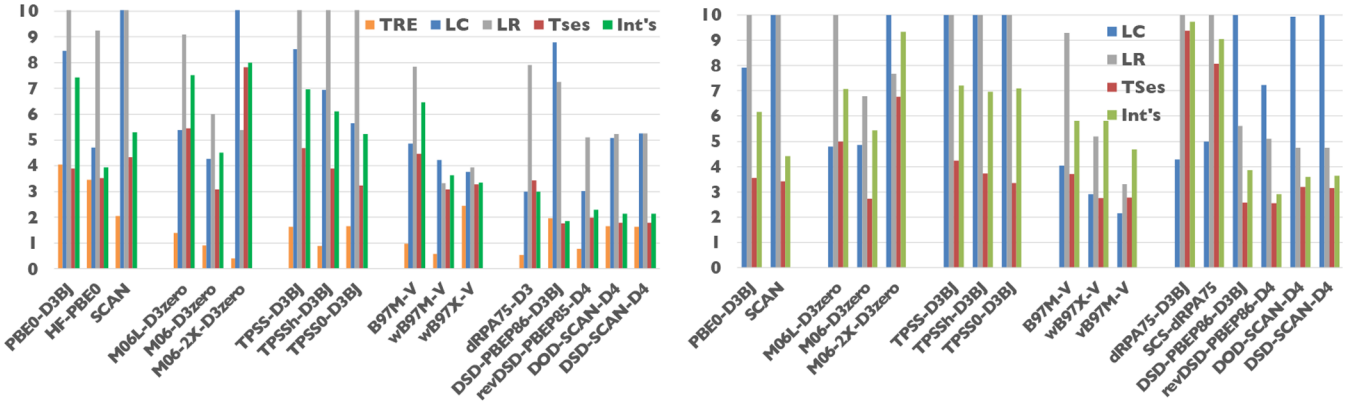

Figure 3. MAD relative to CCSD(T)/def2-TZVPP for different density functionals in the closed-shell (left) and open-shell (right) systems.

One may legitimately ask, then, if one is not engaged in trading the loss of accuracy in DFT for the loss of precision in a highly truncated DLPNO; we definitely recommend TightPNO.

It has been shown[92] that the LNO-CCSD(T) approach of Nagy and Kállay[18,19] as implemented in the MRCC[24] package reproduced canonical CCSD(T) isomer energetics and interconversion barriers of polypyrroles exceptionally well, provided "tight" pair screening settings were applied and in addition `wpairtol=1e-6` was manually specified.[92] (In the mentioned extended porphyrins, the Möbius structures exhibit pronounced static correlation[92] while the Hückel and figure-eight structures do not, hence the relative energies are very sensitive to the correlation treatment. In the present work, as seen in Figure 2 and Tables S10−S13, no appreciable benefit is seen from `wpairtol=1e-6` and the standard Tight setting can be used.) The available implementation is for closed-shell only: in the present work, we also found that LNO-CCSD(T) significantly outperformed the DLPNO-CCSD(T) approach. Thus, for closed-shell **LC** and **LR**, MADs are reduced to 0.35 and 0.16 kcal/mol compared to 2.18 and 0.63 kcal/mol, respectively, for the corresponding DLNPO-CCSD(T_1) calculations. In the latter, the largest deviations (up to 3.44 kcal/mol) for closed-shell **LC** were seen for highly coordinated complexes, especially those with outer-sphere ligands; these deviations do not exceed 0.70 kcal/mol in LNO-CCSD(T) Tight calculations and 1.11 kcal/mol for LR with Normal settings. On average, with the same number of cores of the same CPU type, the LNO-CCSD(T) calculations with these stringent cutoffs ran roughly 3 times as long as the corresponding DLPNO-CCSD(T_1) TightPNO calculations. (See Table S22 in the SI and the Relative Timings of Different Localized Approaches subsection.)

Single-reference second-order Møller−Plesset perturbation theory (MP2) is arguably *the* simplest correlated wave function method. Because it is very vulnerable to static correlation, it unsurprisingly performs poorly and is inferior to most density functionals considered (see below). Canonical and DLPNO-based MP2 methods have very similar MADs of 3.9 and 3.8 kcal/mol, respectively, for the main-group total reaction energies: this indicates that MP2 itself is not compromised by the DLPNO approximation. In the reactions involving Ru(II), the deviations reach 24.73 kcal/mol for **LC**, 8.63 kcal/mol for **LR**, 7.28 kcal/mol for **TS**, and 7.10 kcal/mol for **Int**; as expected, very similar results were obtained using the DLPNO-MP2 approach. In the open-shell systems, the canonical MP2 method gives the largest MAD of 14.96 kcal/mol for the ligand coordination, and this is even worse for the DLPNO-MP2 results (23.84 kcal/mol) because these use a UHF reference rather than the ROHF reference in the canonical MOLPRO calculations, and several of the systems here have very high spin contamination (e.g., $RuCl_3$, $\langle S^2\rangle$ = 1.35). So this is not an issue with the DLPNO approximation *per se*.

The most common ways to improve the performance of MP2 are the orbital-optimized OO-MP2 method[60] and the spin component scaled SCS-MP2 approach,[58,111] a form of spin-component scaling also applied in some double-hybrid functionals.[70−72,112] The OO-MP2 approximation reduces spin contamination in open-shell MP2 calculations and thus is expected to improve energies in difficult cases such as transition states and radicals. We used the resolution of the identity (RI) approximation, which is becoming a *de facto* standard for such calculations and in our systems introduces a negligible (less than 0.05 kcal/mol) deviation. Similar to the 3d transition-metal complexes,[113] the OO-MP2 approximation degrades the MP2 energies in all cases except the open-shell **TSes** (Tables S10−S13).

The SCS-MP2 approach (c_{2ab} = 1.20, c_{2ss} = 0.33) significantly improved the total reaction energies (MAD = 0.15 kcal/mol). It also dramatically reduced the MAD for closed-shell **LC** (to 6.97 kcal/mol) and better than halves the MADs for other closed-shell reactions. A similar, albeit much less dramatic, improvement was seen for the GMTKN55 benchmark suite.[78] In the open-shell systems, the SCS-MP2 results for **LC** and **LR** (10.68 and 4.48 kcal/mol) are slightly better than for plain MP2 (14.96 and 6.97 kcal/mol); however, for **TSes** and **Int's** the SCS-MP2 approach performed worse than plain MP2 (Figure 1 and Tables S10−S13). Interestingly enough, S2-MP2[114] (c_{2ab} = 1.15, c_{2ss} = 0.75) performs comparably to plain MP2.

Hyla-Krispin and Grimme showed,[113] for a set of first-row transition-metal compounds with only mild static correlation, that MP2 always overestimates ligand (CO) coordination energies while SCS-MP2 significantly improves them. Upon close inspection of our results, we observe similar improvements in cases where MP2 energies are overestimated. In these cases, the doublet reference wave functions are not overly spin-contaminated, with $\langle S^2\rangle$ ranging from the ideal 3/4 value to about 1. The spin-component scaling systematically reduces the *overestimated* energies such that a good linear correlation between E[MP2] − E[ref] and E[SCS-MP2] − E[MP2] was found for closed-shell **LC** and **LR;** for open-shell calculations, a statistically meaningful linear correlation is detected when several complexes with high-spin contamination (S^2 > 1) are

https://doi.org/10.1021/acs.jpca.1c05124
J. Phys. Chem. A 2021, 125, 8987−8999

excluded (Figure S7). Similarly, an improvement in the SCS-MP2 energy scales linearly with the *negative* DLPNO-MP2 energy deviation (Figure S8). The reason for such a significant improvement probably lies in the fact (see the spin-component-scaled MP2 review by Grimme, Goerigk, and Fink[111] for a detailed discussion, starting at the end of p. 887) that the same-spin (E_{2SS}) correlation energy is vulnerable to static correlation effects and is overestimated by conventional MP2; the SCS approach throttles this component by a factor of 3. No such dependence was found for the cases of underestimated MP2 energies where the energy deviations mainly arise from opposite-spin (E_{2OS}) correlation, which is primarily short-range and dynamical in character. (See Figures 1 and 2 in ref 111 and the accompanying discussion.) In open-shell calculations, the UHF wave functions of the intermediate complexes are strongly spin-contaminated, with $S^2 > 1$. As far as both closed-shell canonical and DLPNO-based MP2 and open-shell DLPNO-MP2 calculations overestimated **LC** energies, spin-component scaling gives a significant improvement in the total statistic. Only part of the **LR** energies was overestimated (Figure S7), thus the SCS approximation was less beneficial in this case. In open-shell **TSes** and **Int** calculations, errors come to a large extent from an *underestimation* of the interaction energy, thus the influence of the SCS approximation is less pronounced. In these cases, orbital optimization (OO-RI-SCS-MP2) using ORCA slightly improves the total statistics but is still below the performance of canonical MP2. All in all, the accuracy of the RI-SCS-MP2 method is comparable to that of CCSD in closed-shell calculations but is significantly worse in open-shell systems.

Performance of DFT Methods. MAD error statistics with respect to the CCSD(T)/def2-TZVPP results for closed- and open-shell complexes are shown in Figure 3 for the various density functionals. Corresponding RMSD and MSE statistics and similar data calculated with respect to the CCSD(T) and DLPNO-CCSD(T_1)/CBS_{W1} basis set limit estimates can be found in Figures S4−S6 of the Supporting Information. We note that the Berkeley "combinatorially optimized" functionals such as ωB97M-V were parametrized in the presence of the Vydrov−Van Voorhis[115] nonlocal dispersion correction and intrinsically cannot be meaningfully applied without these; others, such as (rev)DSD-PBEP86, DSD-SCAN, and DOD-SCAN, exist in parametrizations with and without dispersion corrections. At a reviewer's request, for other functionals we checked the influence of D3(BJ) and D4 dispersion corrections (Tables S14−S17). In general, D3(BJ) and D4 corrections very similarly affect the performance of the considered functionals, and not in all cases is adding a dispersion correction favorable, especially for open-shell systems. Also, for ligand energies the underlying functional is already overbinding so adding a dispersion correction will only make things worse, but its omission "to make things better" then amounts to reliance on a Pauling point. In particular, we note that SCAN shows smaller deviations from the reference in the absence of D3BJ and D4 corrections in all groups of reactions (e.g., PBE0 in all open-shell complexes). DSD-PBEP86 performs slightly better without the D3BJ dispersion correction in all cases except for closed-shell **TSes**.

As expected, the smallest deviations were found for the overall reaction energies, which involve only main-group elements. The hybrid functionals of the M06 family without dispersion correction (MAD = 0.24 and 0.62 kcal/mol for M06-2X and M06, respectively) and double-hybrid dRPA75-D3 and revDSD-PBEP86-D4 functionals (MAD = 0.53 and 0.73 kcal/mol) show the best performance for this criterion. However, overall, for the considered reaction types in closed- and open-shell complexes, the best results were obtained using the ωB97M-V and ωB97X-V range-separated hybrids as well as the revDSD-PBEP86-D4, DOD-SCAN-D4, and DSD-SCAN-D4 double hybrids, all of which exhibit accuracies between those of DLPNO-CCSD and DLPNO-CCSD(T). Ligand coordination and ligand replacement are the most problematic reactions for most density functionals.

On the third rung (meta-GGA) of Jacob's ladder,[116] B97M-V performs best for all reaction types; however, SCAN without dispersion correction outperforms it for the stabilities of intermediates (MAD = 5.31 vs 6.46 kcal/mol for closed-shell complexes and 4.42 vs 5.81 for open-shell complexes) and is competitive for **TSes** (MAD = 4.34 vs 4.77 and 3.42 vs 3.69 kcal/mol, respectively). TPSS performs almost as well as B97M-V for open-shell **Int's** (MAD = 6.09 kcal/mol).

Adding exact exchange slightly improves the performance of the TPSS and B97M-V functionals. Range-separated hybrids ωB97X-V and ωB97M-V are far superior to other hybrid density functionals. The latter is the best performer for closed-shell **TSes** and **LR** reactions (MAD = 3.08 and 3.32 kcal/mol) and open-shell **LC**, **LR**, and **Int's** (MAD 2.14, 3.30, and 4.69 kcal/mol, respectively), while ωB97X-V was superior to its meta-GGA counterpart for other reactions (MAD = 3.77 and 3.34 kcal/mol for closed-shell **LC** and **Int's** and 2.74 kcal/mol for open-shell **TSes**). Both functionals have their largest absolute errors, in the 6.9−8.8 kcal/mol range, for most Ru(II) reactions, except for **TSes**, for which the errors reach 11.9 kcal/mol. Much larger deviations were found for Ru(III) complexes: 7.9−13.8 kcal/mol **LC**, **LR**, and **TSes** and up to 26.6 kcal/mol for **Int's**. Extrapolation to the complete basis set causes small changes (on the order of 0.6 kcal/mol) in all closed-shell calculations except **LR**, for which the differences reach 1.20 and 1.48 kcal/mol for ωB97X-V and ωB97M-V, respectively; the changes are between 0.1 and 0.8 kcal/mol for most open-shell systems except for **LR** for both functionals and **Int**'s for the latter (MAD values are 3.68, 1.92, and 3.86 kcal/mol, respectively). Other competitive functionals in this group are M06-D3 and PBE0-D3BJ for **TSes** (MAD = 3.09 and 3.89 kcal/mol in closed-shell systems and 2.72 and 3.54 (2.94 without dispersion correction) kcal/mol in open-shell systems); SCAN (the best performer in the group) and M06 for open-shell **Int's** (MAD= 4.42 and 5.22 kcal/mol); and M06-D4 for closed-shell **LC** (MAD = 3.88 kcal/mol). Notably, all pure and hybrid density functionals performed better in the open-shell than in the closed-shell calculations of **TSes**. It is also true for **LC** (except for PBE0, TPSS, and M06 families without dispersion correction) and several functionals (PBE0, SCAN, M06L, and TPSS family without dispersion correction) for **Int's**. Most functionals failed or poorly predicted ligand replacement energies, especially in open-shell complexes.

We checked the performance of density-corrected DFT[68] using the HF-PBE0 functional as an example. Compared to PBE0 without dispersion correction, it appears to be favorable for Ru(II) **LC**, **LR**, **TSes**, and **Int's** and for open-shell **LR** (MAD is reduced from 9.91 to 4.71, from 11.58 to 9.24, from 4.24 to 3.52, from 8.40 to 3.93, and from 12.33 to 11.60 kcal/mol, respectively) while for other open-shell complexes it was detrimental.

On the fifth rung (double hybrids) of Jacob's ladder,[116] the revDSD-PBEP86 functional generally outperforms the original DSD-PBEP86-D3BJ, especially for **LC**. The D4 correction with the revDSD-PBEP86 functional is favorable for all groups of reactions except closed-shell **Int's** and open-shell **TSes**. DOD-

https://doi.org/10.1021/acs.jpca.1c05124
J. Phys. Chem. A 2021, 125, 8987−8999

SCAN-D4 and DSD-SCAN-D4, on the other hand, mostly improved on DSD-PBEP86-D3BJ. However, DSD-PBEP86 performs better without dispersion correction for all groups of reactions except closed-shell **TSes**. On the other hand, DSD-SCAN and DOD-SCAN with D4 correction were better for most groups except for **TSes** and **Int's**. Without dispersion correction, DSD-PBEP86 outperforms DSD-SCAN for all groups except **TRE**. (Optimized DOD-SCAN parameters without dispersion correction are presently not available.) The random phase approximation-based dRPA75 benefits from D3 correction for **TRE**, **LC**, and closed shell **Int's**. In these cases, dRPA75-D3 performs well: MAD = 0.53 kcal/mol for total reaction energies, 2.99 and 4.27 kcal/mol for closed- and open-shell **LC**, and 3.00 kcal/mol for closed-shell **Int's**. Good performance was obtained with dRPA75 without dispersion for closed-shell **LR** and **TSes** (MAD of 3.77 and 2.98 kcal/mol). For Ru(III) systems other than **LC**, it works worse than more conventional double hybrids; SCS-dRPA75 is equivalent to dRPA75-D3 for closed-shell systems, while small improvements are seen for open-shell **LC**, **LR**, and **Int's** but not for **TSes**.

For all density functionals, the highest RMSD and MAD values were found for ligand coordination or ligand replacement reactions. All density functionals overbind ligands in the **LR** reactions (negative MSE), and DOD-SCAN and all DSD double hybrids, PBE0, SCAN, and the TPSS family overbind ligands in **LC** as well. Most functionals (except for SCAN and double hybrids) showed better performance for the ligand coordination reaction in open-shell systems.

Moreover, for transition states and intermediates, (meta)-GGA and hybrid functionals acted better in the open-shell than in the closed-shell calculations; few exceptions were found for **Int's**: ωB97X-V and ωB97M-V performed better in closed-shell systems (MAD of 3.34 and 3.62 vs 5.81 and 4.69 kcal/mol, respectively) and M06 and M06-2X showed very similar accuracy (MAD 4.50 and 7.99 vs 5.43 and 9.34 kcal/mol with the D3 dispersion correction). All functionals except PBE0 and SCAN overestimated the energies of the transition states in open-shell systems (positive MSE, Figures S4−S6). The energies of intermediates are overestimated at all computational levels except for dRPA75 in closed-shell systems and by most functionals (excluding PBE0, the TPSS family, and M06-2X) in open-shell calculations. Therefore, the barrier heights calculated using PBE0, M06L, M06, range-separated, and double hybrid functionals can be surprisingly accurate due to error compensation along a reaction pathway. Future work will focus on static correlation effects[99] in closed- and open-shell complexes, especially on their influence on the barrier heights.

Impact of (4s, 4p) Subvalence Correlation with def2-TZVPP and cc-pwCVTZ-PP Basis Sets. While the 4s and especially 4p orbitals in Ru are close enough to the valence shell that correlating them according to the ORCA "chemical cores" prescription seems chemically sound, combining this with def2-nZVPP basis sets for transition metals appears to be a common practice (e.g., ref 28).

We found in this work (Figure 1 and Table S10) that for the def2-TZVPP basis set the mean absolute effects of the Ru(4s,4p) subvalence correlation on the **LR**, intermediates, and transition states are a nontrivial 1.0 kcal/mol. A similar effect of the subvalence d-orbital correlation (less than 1 kcal/mol) was reported for DLPNO-based calculations on p- and d-block metal halides.[117] However, for **LC**, which causes larger alterations in the Ru electronic structure than ligand replacement, this effect can reach 3.15 and 2.85 kcal/mol for the closed- and open-shell Ru complexes, respectively. The largest deviation in **LR** energies was found for low-coordinated complexes. Thus, for Ru-$(CO)_nCl_2$ the difference between the energies decreases with increasing n = 1...4 from 3.43 to 2.54, 0.76, and finally 0.33 kcal/mol; only for a few Ru(II) complexes with benzene and MA (mostly with outer-sphere Cl ions) do the effects of the Ru(4s,4p) subvalence correlation exceed 1.5 kcal/mol. In contrast, deviations in **LC** energies increase for $Ru(CO)_nCl_2$ from 0.89 to 2.67 and 3.76 kcal/mol with increasing n from 2 to 4 and remain high for benzene and MA complexes (up to 4.72 kcal/mol in complexes with an outer-sphere Cl ion). A similar effect was found in open-shell complexes with stabilization by 2−4.4 kcal/mol due to the correlation of Ru(4s,4p) orbitals found for most carbonyl complexes. In the weaker crystal field of water ligands, the influence of subvalence orbital correlation is smaller, up to 2.62 kcal/mol in CO-free and monocarbonyl water complexes. For closed-shell transition states, the difference reaches 3.0−3.9 kcal/mol in several cases; for open-shell **TSes**, the largest deviation is much smaller, mostly within 1.5 kcal/mol. Among the intermediates, the largest deviation of 4.59 and 3.34 kcal/mol was found for the low-coordinated closed-shell **Int3-CO1** and open-shell **MA-Int1**, respectively.

A reviewer, however, pointed out that these basis sets may be insufficiently flexible in the core−valence boundary region, which might lead to overestimation due to basis set superposition error. While a recalculation of all of the canonical CCSD(T)s with the cc-pwCVTZ-PP basis set on Ru and cc-pVTZ on other elements was not practical within resource constraints, we did make this comparison for the most sensitive **LC** and **LR** subsets of closed-shell systems. The details can be found in Table S23.

First, a direct comparison between def2-TZVPP and cc-pwCVTZ-PP is somewhat obscured by the fact that these basis sets use different ECPs (fitted to Wood−Boring and Dirac−Fock atomic calculations, respectively), as becomes plain when comparing HF/def2-QZVPP, HF/dhf-QZVPP, and HF/cc-pVQZ,Ru=cc-pwCVQZ-PP. We could hence approximately halve the discrepancy between CCSD(T)/def2-TZVPP and CCSD(T)/cc-pVTZ,Ru=cc-pwCVTZ-PP simply by switching to dhf-TZVPP, but then one would have to make the corresponding change to all of the localized orbital and DFT calculations.

A more pertinent comparison between the two basis sets would be for the (4s,4p) correlation contributions obtained as the difference between CCSD(T) calculations with and without these orbitals frozen. We then find (Table S23) that for ligand coordination, discrepancies can increase to 1 and occasionally even 2 kcal/mol when strong changes in the Ru(II) electronic structure take place, as in the cases of benzene coordination with Ru(CO)Cl2 and MA replacement of the chloride ion in the inner coordination sphere of $Ru(CO)_4Cl_2$. For ligand replacement, a degree of cancellation across the reaction takes place and the discrepancies are more modest. It is reasonable to assume that the same would happen to barrier heights and intermediates.

This issue is obviously much broader than Ru complexes and will be addressed in more detail in an upcoming paper on the MOBH35 benchmark data set (Semidalas, E.; Efremenko, I.; Martin, J. M. L. In preparation).

Relative Timings of Different Localized Approaches. Even when jobs are run on identical hardware configurations, wall clock times can be subject to mild variation because of variable clock speeds and "thermal throttling" of modern

https://doi.org/10.1021/acs.jpca.1c05124
J. Phys. Chem. A 2021, 125, 8987−8999

processors and possible local variations in the latter due to uneven temperature distribution inside the data center. That reservation having been stated, we were able to extract wall clock timing data for six jobs on identical hardware configurations, namely, all 16 cores of twin Intel(R) Xeon(R) CPU E5-2630 v3 processors with a 2.40 GHz base clock speed, 256 GB of RAM, and 4TB worth of striped solid-state disk. (The latter is relevant for DLPNO-CCSD(T_1), which is somewhat I/O bandwidth-hungry.) Table S22 in the SI contains wall clock timing data for five different calculations with the def2-TZVPP basis set (LNO-CCSD(T) Normal, LNO-CCSD(T) Tight, DLPNO-CCSD(T) NormalPNO, ditto TightPNO, and DLPNO_CCSD(T_1) TightPNO). For the systems at hand, LNO Tight jobs on average ran 4.3 times as long as their Normal equivalents. Running LNO-CCSD(T) with the `wpairtol=1e-6` option yields very similar results to the Tight option and requires a very similar run time. DLPNO-CCSD(T) TightPNO is an average of 5.2 times as long as NormalPNO, and DLPNO-CCSD(T_1) TightPNO is an average of 1.9 times as long as its (T0) counterparts. Finally, LNO-CCSD(T) Tight ran on average 3.1 times as long as DLPNO-CCSD(T_1) TightPNO. While somewhat different ratios may be obtained for other systems, to us the extra computational expense seems to be commensurate with the increase in accuracy.

CONCLUSIONS

The results presented in this work demonstrate that the DLPNO-CCSD(T_1) approximation with TightPNO cutoffs closely reproduces the canonical CCSD(T) results for Ru(II) complexes, with the largest MAD (2.18 kcal/mol) found for ligand coordination reactions. For open-shell Ru(III) complexes, the DLPNO-CCSD(T_1) TightPNO approach fortuitously showed better performance for **LC** than its closed-shell equivalent (MAD = 1.34 kcal/mol) and closely reproduced other types of energetics, with the largest MAD of 2.06 kcal/mol found for the energies of intermediates.

Furthermore, the LNO-CCSD(T) approach of Nagy and Kállay with Tight cutoffs reproduces canonical CCSD(T) very closely for closed-shell **LC** and **LR** reactions (MAD of 0.35 and 0.16 kcal/mol, respectively) at the expense of roughly tripling the computational time. This approach is recommended for closed-shell transition-metal complexes, with an open-shell implementation not yet being available.

Our findings concerning the performance of density functionals in closed-shell systems are consistent with the observations of Najibi and Goerigk[118] and ourselves[72,78] for the very large GMTKN55 main-group benchmark[36] and of Iron and Janes[28,29] for the MOBH35 transition-metal reaction benchmark, in particular, (a) that range-separated hybrids ωB97X-V and ωB97M-V acquit themselves particularly well; (b) that revDSD represents an improvement over the original DSD not just for the main group but also for transition metals; and (c) that, unlike for the main group where empirical double hybrids are clearly superior, they offer no clear advantage over ωB97M-V and ωB97X-V for transition-metal reactions. In agreement with Iron and Janes,[28,29] who found the new DSD-SCAN double hybrid[72] to be among the best performers for MOBH35, we find it to be competitive with revDSD-PBEP86 and the ωB97*n*-V family for the present problem; DOD-SCAN has very similar accuracy.

Pure and hybrid functionals (rungs 3 and 4 of Jacob's ladder) showed better performance in the open-shell than in closed-shell calculations for the energies of ligand coordination, transition states, and intermediates. In contrast, double hybrids performed worse for open-shell systems, especially for the energies of ligand coordination.

In the larger scheme of things, while for this representative late-transition-metal homogeneous catalysis problem DLPNO-CCSD(T) with TightPNO cutoffs is definitely superior in accuracy to the best available DFT methods, it is about 2 orders of magnitude more expensive computationally, albeit drastically cheaper than the canonical CCSD(T) reference calculations. For closed-shell cases, LNO-CCSD(T) with "Tight" cutoffs can be used as a substitute for the canonical calculations. (Unlike for the highly extended polypyrrol systems in ref 92, where `wpairtol=1e-6` significantly further enhanced accuracy, this setting has no significant effect on the present problem.)

ASSOCIATED CONTENT

Supporting Information

. The Supporting Information is available free of charge at https://pubs.acs.org/doi/10.1021/acs.jpca.1c05124.

Tables and figures containing parameters discussed in the main text (PDF)

HF, MP2, CCSD, and CCSD(T) total energies for the canonical CCSD(T) calculations (XLSX)

ZIP archive with all PBE0-D3BJ/def2-TZVP optimized structures as Cartesian coordinate files (*XYZ*, in Å) (ZIP)

AUTHOR INFORMATION

Corresponding Authors

Irena Efremenko − *Department of Molecular Chemistry and Materials Science, Weizmann Institute of Science, 7610001 Rehovot, Israel*; Email: irena.efremenko@weizmann.ac.il

Jan M. L. Martin − *Department of Molecular Chemistry and Materials Science, Weizmann Institute of Science, 7610001 Rehovot, Israel*; orcid.org/0000-0002-0005-5074; Email: gershom@weizmann.ac.il

Complete contact information is available at: https://pubs.acs.org/10.1021/acs.jpca.1c05124

Notes

A rough early draft of the closed-shell part of this study was published earlier in extended abstract form[10] in the proceedings of the 2019 International Conference on Computational Materials Science and Engineerings (ICCMSE-2019).
The authors declare no competing financial interest.

ACKNOWLEDGMENTS

This research was supported by the Israel Science Foundation (grant 1969/20), the Minerva Foundation (grant 2020/05), and the Helen and Martin Kimmel Center for Molecular Design (Weizmann Institute of Science).

REFERENCES

(1) Murai, S.; Kakiuchi, F.; Sekine, S.; Tanaka, Y.; Kamatani, A.; Sonoda, M.; Chatani, N. Efficient Catalytic Addition of Aromatic Carbon-Hydrogen Bonds to Olefins. *Nature* **1993**, *366*, 529−531.

(2) Kischel, J.; Jovel, I.; Mertins, K.; Zapf, A.; Beller, M. A Convenient FeCl3 -Catalyzed Hydroarylation of Styrenes. *Org. Lett.* **2006**, *8*, 19−22.

(3) Zhong, H. A.; Labinger, J. A.; Bercaw, J. E. C−H Bond Activation by Cationic Platinum(II) Complexes: Ligand Electronic and Steric Effects. *J. Am. Chem. Soc.* **2002**, *124*, 1378−1399.

(4) Jia, C.; Piao, D.; Oyamada, J.; Lu, W.; Kitamura, T.; Fujiwara, Y. Efficient Activation of Aromatic C-H Bonds for Addition to C-C Multiple Bonds. *Science (Washington, DC, U. S.)* **2000**, *287*, 1992−1995.
(5) *From C-H to C-C Bonds*; Li, C.-J., Ed.; Green Chemistry Series; Royal Society of Chemistry: Cambridge, 2014.
(6) Burke, A. J.; Marques, C. S. *Catalytic Arylation Methods: From the Academic Lab to Industrial Processes*; Wiley, 2015.
(7) Kakiuchi, F.; Sato, T.; Yamauchi, M.; Chatani, N.; Murai, S. Ruthenium-Catalyzed Coupling of Aromatic Carbon-Hydrogen Bonds in Aromatic Imidates with Olefins. *Chem. Lett.* **1999**, *28*, 19−20.
(8) Weissman, H.; Song, X.; Milstein, D. Ru-Catalyzed Oxidative Coupling of Arenes with Olefins Using O 2. *J. Am. Chem. Soc.* **2001**, *123*, 337−338.
(9) Milstein, D. Challenging Metal-Based Transformations. From Single-Bond Activation to Catalysis and Metallaquinonoids. *Pure Appl. Chem.* **2003**, *75*, 445−460.
(10) Efremenko, I.; Martin, J. M. L. Coupled Cluster Benchmark of New Density Functionals and Domain Pair Natural Orbital Methods: Mechanisms of Hydroarylation and Oxidative Coupling Catalyzed by Ru(II) Chloride Carbonyls. *AIP Conf. Proc.* **2019**, *2186*, 030005.
(11) Shavitt, I.; Bartlett, R. J. *Many-Body Methods in Chemistry and Physics*; Cambridge University Press: Cambridge, U.K., 2009.
(12) Purvis, G. D.; Bartlett, R. J. A Full Coupled-cluster Singles and Doubles Model: The Inclusion of Disconnected Triples. *J. Chem. Phys.* **1982**, *76*, 1910−1918.
(13) Raghavachari, K.; Trucks, G. W.; Pople, J. A.; Head-Gordon, M. A Fifth-Order Perturbation Comparison of Electron Correlation Theories. *Chem. Phys. Lett.* **1989**, *157*, 479−483.
(14) Watts, J. D.; Gauss, J.; Bartlett, R. J. Coupled-Cluster Methods with Noniterative Triple Excitations for Restricted Open-Shell Hartree−Fock and Other General Single Determinant Reference Functions. Energies and Analytical Gradients. *J. Chem. Phys.* **1993**, *98*, 8718−8733.
(15) Riplinger, C.; Neese, F. An Efficient and near Linear Scaling Pair Natural Orbital Based Local Coupled Cluster Method. *J. Chem. Phys.* **2013**, *138*, 034106.
(16) Riplinger, C.; Sandhoefer, B.; Hansen, A.; Neese, F. Natural Triple Excitations in Local Coupled Cluster Calculations with Pair Natural Orbitals. *J. Chem. Phys.* **2013**, *139*, 134101.
(17) Ma, Q.; Werner, H.-J. Explicitly Correlated Local Coupled-Cluster Methods Using Pair Natural Orbitals. *Wiley Interdiscip. Rev.: Comput. Mol. Sci.* **2018**, *8*, e1371.
(18) Nagy, P. R.; Kállay, M. Approaching the Basis Set Limit of CCSD(T) Energies for Large Molecules with Local Natural Orbital Coupled-Cluster Methods. *J. Chem. Theory Comput.* **2019**, *15*, 5275−5298.
(19) Nagy, P. R.; Samu, G.; Kállay, M. Optimization of the Linear-Scaling Local Natural Orbital CCSD(T) Method: Improved Algorithm and Benchmark Applications. *J. Chem. Theory Comput.* **2018**, *14*, 4193−4215.
(20) Liakos, D. G.; Guo, Y.; Neese, F. Comprehensive Benchmark Results for the Domain Based Local Pair Natural Orbital Coupled Cluster Method (DLPNO-CCSD(T)) for Closed- and Open-Shell Systems. *J. Phys. Chem. A* **2020**, *124*, 90−100.
(21) Semidalas, E.; Martin, J. M. L. Canonical and DLPNO-Based Composite Wavefunction Methods Parametrized against Large and Chemically Diverse Training Sets. 2: Correlation-Consistent Basis Sets, Core−Valence Correlation, and F12 Alternatives. *J. Chem. Theory Comput.* **2020**, *16*, 7507−7524.
(22) Ma, Q.; Werner, H.-J. Scalable Electron Correlation Methods. 8. Explicitly Correlated Open-Shell Coupled-Cluster with Pair Natural Orbitals PNO-RCCSD(T)-F12 and PNO-UCCSD(T)-F12. *J. Chem. Theory Comput.* **2021**, *17*, 902−926.
(23) Szabó, P. B.; Csóka, J.; Kállay, M.; Nagy, P. R. Linear-Scaling Open-Shell MP2 Approach: Algorithm, Benchmarks, and Large-Scale Applications. *J. Chem. Theory Comput.* **2021**, *17*, 2886−2905.
(24) Kállay, M.; Nagy, P. R.; Mester, D.; Rolik, Z.; Samu, G.; Csontos, J.; Csóka, J.; Szabó, P. B.; Gyevi-Nagy, L.; Hégely, B.; et al. The MRCC Program System: Accurate Quantum Chemistry from Water to Proteins. *J. Chem. Phys.* **2020**, *152*, 074107.
(25) Anacker, T.; Tew, D. P.; Friedrich, J. First UHF Implementation of the Incremental Scheme for Open-Shell Systems. *J. Chem. Theory Comput.* **2016**, *12*, 65−78.
(26) Zhang, J.; Dolg, M. Third-Order Incremental Dual-Basis Set Zero-Buffer Approach for Large High-Spin Open-Shell Systems. *J. Chem. Theory Comput.* **2015**, *11*, 962−968.
(27) Dohm, S.; Hansen, A.; Steinmetz, M.; Grimme, S.; Checinski, M. P. Comprehensive Thermochemical Benchmark Set of Realistic Closed-Shell Metal Organic Reactions. *J. Chem. Theory Comput.* **2018**, *14*, 2596−2608.
(28) Iron, M. A.; Janes, T. Evaluating Transition Metal Barrier Heights with the Latest Density Functional Theory Exchange−Correlation Functionals: The MOBH35 Benchmark Database. *J. Phys. Chem. A* **2019**, *123*, 3761−3781.
(29) Iron, M. A.; Janes, T. Correction to "Evaluating Transition Metal Barrier Heights with the Latest Density Functional Theory Exchange−Correlation Functionals: The MOBH35 Benchmark Database. *J. Phys. Chem. A* **2019**, *123*, 6379−6380.
(30) Shiekh, B. A. Hierarchy of Commonly Used DFT Methods for Predicting the Thermochemistry of Rh-Mediated Chemical Transformations. *ACS Omega* **2019**, *4*, 15435−15443.
(31) Rohmann, K.; Hölscher, M.; Leitner, W. Can Contemporary Density Functional Theory Predict Energy Spans in Molecular Catalysis Accurately Enough To Be Applicable for in Silico Catalyst Design? A Computational/Experimental Case Study for the Ruthenium-Catalyzed Hydrogenation of Olefins. *J. Am. Chem. Soc.* **2016**, *138*, 433−443.
(32) Kang, R.; Yao, J.; Chen, H. Are DFT Methods Accurate in Mononuclear Ruthenium-Catalyzed Water Oxidation? An Ab Initio Assessment. *J. Chem. Theory Comput.* **2013**, *9*, 1872−1879.
(33) Piacenza, M.; Hyla-Kryspin, I.; Grimme, S. A Comparative Quantum Chemical Study of the Ruthenium Catalyzed Olefin Metathesis. *J. Comput. Chem.* **2007**, *28*, 2275−2285.
(34) Zhao, Y.; Truhlar, D. G. Benchmark Energetic Data in a Model System for Grubbs II Metathesis Catalysis and Their Use for the Development, Assessment, and Validation of Electronic Structure Methods. *J. Chem. Theory Comput.* **2009**, *5*, 324−333.
(35) Sun, Y.; Hu, L.; Chen, H. Comparative Assessment of DFT Performances in Ru- and Rh-Promoted σ-Bond Activations. *J. Chem. Theory Comput.* **2015**, *11*, 1428−1438.
(36) Goerigk, L.; Hansen, A.; Bauer, C.; Ehrlich, S.; Najibi, A.; Grimme, S. A Look at the Density Functional Theory Zoo with the Advanced GMTKN55 Database for General Main Group Thermochemistry, Kinetics and Noncovalent Interactions. *Phys. Chem. Chem. Phys.* **2017**, *19*, 32184−32215.
(37) Guo, Y.; Riplinger, C.; Becker, U.; Liakos, D. G.; Minenkov, Y.; Cavallo, L.; Neese, F. Communication: An Improved Linear Scaling Perturbative Triples Correction for the Domain Based Local Pair-Natural Orbital Based Singles and Doubles Coupled Cluster Method [DLPNO-CCSD(T)]. *J. Chem. Phys.* **2018**, *148*, 011101.
(38) Guo, Y.; Riplinger, C.; Liakos, D. G.; Becker, U.; Saitow, M.; Neese, F. Linear Scaling Perturbative Triples Correction Approximations for Open-Shell Domain-Based Local Pair Natural Orbital Coupled Cluster Singles and Doubles Theory [DLPNO-CCSD(T0/T)]. *J. Chem. Phys.* **2020**, *152*, 024116.
(39) Feldt, M.; Phung, Q. M.; Pierloot, K.; Mata, R. A.; Harvey, J. N. Limits of Coupled-Cluster Calculations for Non-Heme Iron Complexes. *J. Chem. Theory Comput.* **2019**, *15*, 922−937.
(40) Feldt, M.; Martín-Fernández, C.; Harvey, J. N. Energetics of Non-Heme Iron Reactivity: Can: Ab Initio Calculations Provide the Right Answer? *Phys. Chem. Chem. Phys.* **2020**, *22*, 23908−23919.
(41) Flöser, B. M.; Guo, Y.; Riplinger, C.; Tuczek, F.; Neese, F. Detailed Pair Natural Orbital-Based Coupled Cluster Studies of Spin Crossover Energetics. *J. Chem. Theory Comput.* **2020**, *16*, 2224−2235.
(42) Weigend, F.; Ahlrichs, R. Balanced Basis Sets of Split Valence, Triple Zeta Valence and Quadruple Zeta Valence Quality for H to Rn:

https://doi.org/10.1021/acs.jpca.1c05124
J. Phys. Chem. A 2021, 125, 8987−8999

Design and Assessment of Accuracy. *Phys. Chem. Chem. Phys.* **2005**, *7*, 3297−3305.
(43) Adamo, C.; Barone, V. Toward Reliable Density Functional Methods without Adjustable Parameters: The PBE0Model. *J. Chem. Phys.* **1999**, *110*, 6158−6170.
(44) Grimme, S.; Ehrlich, S.; Goerigk, L. Effect of the Damping Function in Dispersion Corrected Density Functional Theory. *J. Comput. Chem.* **2011**, *32*, 1456−1465.
(45) Perdew, J.; Burke, K.; Ernzerhof, M. Generalized Gradient Approximation Made Simple. *Phys. Rev. Lett.* **1996**, *77*, 3865−3868.
(46) Frisch, M. J.; Trucks, G. W.; Schlegel, H. B.; Scuseria, G. E.; Robb, M. A.; Cheeseman, J. R.; Scalmani, G.; Barone, V.; Petersson, G. A.; Nakatsuji, H.; et al. *Gaussian 16*, Revision C.01; Gaussian, Inc.: Wallingford, CT, 2016.
(47) Werner, H.-J.; Knowles, P. J.; Manby, F. R.; Black, J. A.; Doll, K.; Heßelmann, A.; Kats, D.; Köhn, A.; Korona, T.; Kreplin, D. A.; et al. The Molpro Quantum Chemistry Package. *J. Chem. Phys.* **2020**, *152*, 144107.
(48) Saitow, M.; Becker, U.; Riplinger, C.; Valeev, E. F.; Neese, F. A New Near-Linear Scaling, Efficient and Accurate, Open-Shell Domain-Based Local Pair Natural Orbital Coupled Cluster Singles and Doubles Theory. *J. Chem. Phys.* **2017**, *146*, 164105.
(49) Neese, F.; Wennmohs, F.; Becker, U.; Riplinger, C. The ORCA Quantum Chemistry Program Package. *J. Chem. Phys.* **2020**, *152*, 224108.
(50) Hellweg, A.; Hättig, C.; Höfener, S.; Klopper, W. Optimized Accurate Auxiliary Basis Sets for RI-MP2 and RI-CC2 Calculations for the Atoms Rb to Rn. *Theor. Chem. Acc.* **2007**, *117*, 587−597.
(51) Weigend, F.; Häser, M.; Patzelt, H.; Ahlrichs, R. RI-MP2: Optimized Auxiliary Basis Sets and Demonstration of Efficiency. *Chem. Phys. Lett.* **1998**, *294*, 143−152.
(52) Weigend, F. Hartree−Fock Exchange Fitting Basis Sets for H to Rn. *J. Comput. Chem.* **2008**, *29*, 167−175.
(53) Andrae, D.; Häußermann, U.; Dolg, M.; Stoll, H.; Preuss, H. Energy-Adjustedab Initio Pseudopotentials for the Second and Third Row Transition Elements. *Theor. Chim. Acta* **1990**, *77*, 123−141.
(54) Williams, T. G.; DeYonker, N. J.; Wilson, A. K. Hartree-Fock Complete Basis Set Limit Properties for Transition Metal Diatomics. *J. Chem. Phys.* **2008**, *128*, 044101.
(55) Neese, F.; Valeev, E. F. Revisiting the Atomic Natural Orbital Approach for Basis Sets: Robust Systematic Basis Sets for Explicitly Correlated and Conventional Correlated Ab Initio Methods? *J. Chem. Theory Comput.* **2011**, *7*, 33−43.
(56) Liakos, D. G.; Sparta, M.; Kesharwani, M. K.; Martin, J. M. L.; Neese, F. Exploring the Accuracy Limits of Local Pair Natural Orbital Coupled-Cluster Theory. *J. Chem. Theory Comput.* **2015**, *11*, 1525−1539.
(57) Pinski, P.; Riplinger, C.; Valeev, E. F.; Neese, F. Sparse Maps - A Systematic Infrastructure for Reduced-Scaling Electronic Structure Methods. I. An Efficient and Simple Linear Scaling Local MP2 Method That Uses an Intermediate Basis of Pair Natural Orbitals. *J. Chem. Phys.* **2015**, *143*, 034108.
(58) Grimme, S. Improved Second-Order Møller−Plesset Perturbation Theory by Separate Scaling of Parallel- and Antiparallel-Spin Pair Correlation Energies. *J. Chem. Phys.* **2003**, *118*, 9095−9102.
(59) Lochan, R. C.; Head-Gordon, M. Orbital-Optimized Opposite-Spin Scaled Second-Order Correlation: An Economical Method to Improve the Description of Open-Shell Molecules. *J. Chem. Phys.* **2007**, *126*, 164101.
(60) Neese, F.; Schwabe, T.; Kossmann, S.; Schirmer, B.; Grimme, S. Assessment of Orbital-Optimized, Spin-Component Scaled Second-Order Many-Body Perturbation Theory for Thermochemistry and Kinetics. *J. Chem. Theory Comput.* **2009**, *5*, 3060−3073.
(61) Mardirossian, N.; Head-Gordon, M. Mapping the Genome of Meta-Generalized Gradient Approximation Density Functionals: The Search for B97M-V. *J. Chem. Phys.* **2015**, *142*, 074111.
(62) Mardirossian, N.; Head-Gordon, M. ωB97X-V: A 10-Parameter, Range-Separated Hybrid, Generalized Gradient Approximation Density Functional with Nonlocal Correlation, Designed by a Survival-of-the-Fittest Strategy. *Phys. Chem. Chem. Phys.* **2014**, *16*, 9904−9924.
(63) Mardirossian, N.; Head-Gordon, M. ωB97M-V: A Combinatorially Optimized, Range-Separated Hybrid, Meta-GGA Density Functional with VV10 Nonlocal Correlation. *J. Chem. Phys.* **2016**, *144*, 214110.
(64) Zhao, Y.; Truhlar, D. G. A New Local Density Functional for Main-Group Thermochemistry, Transition Metal Bonding, Thermochemical Kinetics, and Noncovalent Interactions. *J. Chem. Phys.* **2006**, *125*, 194101.
(65) Zhao, Y.; Truhlar, D. G. The M06 Suite of Density Functionals for Main Group Thermochemistry, Thermochemical Kinetics, Noncovalent Interactions, Excited States, and Transition Elements: Two New Functionals and Systematic Testing of Four M06-Class Functionals and 12 Other Function. *Theor. Chem. Acc.* **2008**, *120*, 215−241.
(66) Tao, J.; Perdew, J.; Staroverov, V.; Scuseria, G. Climbing the Density Functional Ladder: Nonempirical Meta−Generalized Gradient Approximation Designed for Molecules and Solids. *Phys. Rev. Lett.* **2003**, *91*, 146401.
(67) Grimme, S. Accurate Calculation of the Heats of Formation for Large Main Group Compounds with Spin-Component Scaled MP2 Methods. *J. Phys. Chem. A* **2005**, *109*, 3067−3077.
(68) Wasserman, A.; Nafziger, J.; Jiang, K.; Kim, M.-C.; Sim, E.; Burke, K. The Importance of Being Inconsistent. *Annu. Rev. Phys. Chem.* **2017**, *68*, 555−581.
(69) Santra, G.; Cho, M.; Martin, J. M. L. Exploring Avenues beyond Revised DSD Functionals: I. Range Separation, with x DSD as a Special Case. *J. Phys. Chem. A* **2021**, *125*, 4614−4627.
(70) Kozuch, S.; Martin, J. M. L. DSD-PBEP86: In Search of the Best Double-Hybrid DFT with Spin-Component Scaled MP2 and Dispersion Corrections. *Phys. Chem. Chem. Phys.* **2011**, *13*, 20104.
(71) Kozuch, S.; Martin, J. M. L. Spin-Component-Scaled Double Hybrids: An Extensive Search for the Best Fifth-Rung Functionals Blending DFT and Perturbation Theory. *J. Comput. Chem.* **2013**, *34*, 2327−2344.
(72) Santra, G.; Sylvetsky, N.; Martin, J. M. L. Minimally Empirical Double-Hybrid Functionals Trained against the GMTKN55 Database: revDSD-PBEP86-D4, revDOD-PBE-D4, and DOD-SCAN-D4. *J. Phys. Chem. A* **2019**, *123*, 5129−5143.
(73) Grimme, S.; Antony, J.; Ehrlich, S.; Krieg, H. A Consistent and Accurate Ab Initio Parametrization of Density Functional Dispersion Correction (DFT-D) for the 94 Elements H-Pu. *J. Chem. Phys.* **2010**, *132*, 154104.
(74) Caldeweyher, E.; Ehlert, S.; Hansen, A.; Neugebauer, H.; Spicher, S.; Bannwarth, C.; Grimme, S. A Generally Applicable Atomic-Charge Dependent London Dispersion Correction. *J. Chem. Phys.* **2019**, *150*, 154122.
(75) Grimme, S. Semiempirical Hybrid Density Functional with Perturbative Second-Order Correlation. *J. Chem. Phys.* **2006**, *124*, 034108.
(76) Goerigk, L.; Grimme, S. Double-Hybrid Density Functionals. *Wiley Interdiscip. Rev. Comput. Mol. Sci.* **2014**, *4*, 576−600.
(77) Brémond, E.; Ciofini, I.; Sancho-García, J. C.; Adamo, C. Nonempirical Double-Hybrid Functionals: An Effective Tool for Chemists. *Acc. Chem. Res.* **2016**, *49*, 1503−1513.
(78) Martin, J. M. L.; Santra, G. Empirical Double-Hybrid Density Functional Theory: A 'Third Way' in Between WFT and DFT. *Isr. J. Chem.* **2020**, *60*, 787−804.
(79) Halkier, A.; Helgaker, T.; Jørgensen, P.; Klopper, W.; Koch, H.; Olsen, J.; Wilson, A. K. Basis-Set Convergence in Correlated Calculations on Ne, N_2, and H_2O. *Chem. Phys. Lett.* **1998**, *286*, 243−252.
(80) Kossmann, S.; Neese, F. Efficient Structure Optimization with Second-Order Many-Body Perturbation Theory: The RIJCOSX-MP2Method. *J. Chem. Theory Comput.* **2010**, *6*, 2325−2338.
(81) Neese, F.; Wennmohs, F.; Hansen, A.; Becker, U. Efficient, Approximate and Parallel Hartree-Fock and Hybrid DFT Calculations. A "Chain-of-Spheres" Algorithm for the Hartree-Fock Exchange. *Chem. Phys.* **2009**, *356*, 98−109.

https://doi.org/10.1021/acs.jpca.1c05124
J. Phys. Chem. A 2021, 125, 8987−8999

(82) Bernholdt, D. E. Scalability of Correlated Electronic Structure Calculations on Parallel Computers: A Case Study of the RI-MP2 Method. *Parallel Comput.* **2000**, *26*, 945−963.
(83) Vahtras, O.; Almlöf, J.; Feyereisen, M. W. Integral Approximations for LCAO-SCF Calculations. *Chem. Phys. Lett.* **1993**, *213*, 514−518.
(84) Feyereisen, M.; Fitzgerald, G.; Komornicki, A. Use of Approximate Integrals in Ab Initio Theory. An Application in MP2 Energy Calculations. *Chem. Phys. Lett.* **1993**, *208*, 359−363.
(85) Bernholdt, D. E.; Harrison, R. J. Large-Scale Correlated Electronic Structure Calculations: The RI-MP2Method on Parallel Computers. *Chem. Phys. Lett.* **1996**, *250*, 477−484.
(86) Kendall, R. A.; Früchtl, H. A. The Impact of the Resolution of the Identity Approximate Integral Method on Modern Ab Initio Algorithm Development. *Theor. Chem. Acc.* **1997**, *97*, 158−163.
(87) Weigend, F. Accurate Coulomb-Fitting Basis Sets for H to Rn. *Phys. Chem. Chem. Phys.* **2006**, *8*, 1057−1065.
(88) Hättig, C. Optimization of Auxiliary Basis Sets for RI-MP2 and RI-CC2 Calculations: Core−Valence and Quintuple-ζ Basis Sets for H to Ar and QZVPP Basis Sets for Li to Kr. *Phys. Chem. Chem. Phys.* **2005**, *7*, 59−66.
(89) Brauer, B.; Kesharwani, M. K.; Kozuch, S.; Martin, J. M. L. The S66 × 8 Benchmark for Noncovalent Interactions Revisited: Explicitly Correlated Ab Initio Methods and Density Functional Theory. *Phys. Chem. Chem. Phys.* **2016**, *18*, 20905−20925.
(90) Mezei, P. D.; Csonka, G. I.; Ruzsinszky, A.; Kállay, M. Construction and Application of a New Dual-Hybrid Random Phase Approximation. *J. Chem. Theory Comput.* **2015**, *11*, 4615−4626.
(91) Mezei, P. D.; Csonka, G. I.; Ruzsinszky, A.; Kállay, M. Construction of a Spin-Component Scaled Dual-Hybrid Random Phase Approximation. *J. Chem. Theory Comput.* **2017**, *13*, 796−803.
(92) Sylvetsky, N.; Banerjee, A.; Alonso, M.; Martin, J. M. L. Performance of Localized Coupled Cluster Methods in a Moderately Strong Correlation Regime: Hückel−Möbius Interconversions in Expanded Porphyrins. *J. Chem. Theory Comput.* **2020**, *16*, 3641−3653.
(93) Peterson, K. A.; Figgen, D.; Dolg, M.; Stoll, H. Energy-Consistent Relativistic Pseudopotentials and Correlation Consistent Basis Sets for the 4d Elements Y−Pd. *J. Chem. Phys.* **2007**, *126*, 124101.
(94) Dunning, T. H. Gaussian Basis Sets for Use in Correlated Molecular Calculations. I. The Atoms Boron through Neon and Hydrogen. *J. Chem. Phys.* **1989**, *90*, 1007−1023.
(95) Chan, B.; Karton, A.; Raghavachari, K.; Radom, L. Heats of Formation for CrO, CrO2, and CrO3 : An Extreme Challenge for Black-Box Composite Procedures. *J. Chem. Theory Comput.* **2012**, *8*, 3159−3166.
(96) Jiang, W.; DeYonker, N. J.; Wilson, A. K. Multireference Character for 3d Transition-Metal-Containing Molecules. *J. Chem. Theory Comput.* **2012**, *8*, 460−468.
(97) Chan, B.; Gill, P. M. W.; Kimura, M. Assessment of DFT Methods for Transition Metals with the TMC151 Compilation of Data Sets and Comparison with Accuracies for Main-Group Chemistry. *J. Chem. Theory Comput.* **2019**, *15*, 3610−3622.
(98) Wang, J.; Manivasagam, S.; Wilson, A. K. Multireference Character for 4d Transition Metal-Containing Molecules. *J. Chem. Theory Comput.* **2015**, *11*, 5865−5872.
(99) Hollett, J. W.; Gill, P. M. W. The Two Faces of Static Correlation. *J. Chem. Phys.* **2011**, *134*, 114111.
(100) Scuseria, G. E.; Tsuchimochi, T. Constrained-Pairing Mean-Field Theory. II. Exact Treatment of Dissociations to Nondegenerate Orbitals. *J. Chem. Phys.* **2009**, *131*, 164119.
(101) Husch, T.; Freitag, L.; Reiher, M. Calculation of Ligand Dissociation Energies in Large Transition-Metal Complexes. *J. Chem. Theory Comput.* **2018**, *14*, 2456−2468.
(102) Aoto, Y. A.; de Lima Batista, A. P.; Köhn, A.; de Oliveira-Filho, A. G. S. How To Arrive at Accurate Benchmark Values for Transition Metal Compounds: Computation or Experiment? *J. Chem. Theory Comput.* **2017**, *13*, 5291−5316.
(103) Fogueri, U. R.; Kozuch, S.; Karton, A.; Martin, J. M. L. A Simple DFT-Based Diagnostic for Nondynamical Correlation. *Theor. Chem. Acc.* **2013**, *132*, 1291.
(104) Lee, T. J.; Taylor, P. R. A Diagnostic for Determining the Quality of Single-Reference Electron Correlation Methods. *Int. J. Quantum Chem.* **1989**, *36*, 199−207.
(105) Janssen, C. L.; Nielsen, I. M. B. New Diagnostics for Coupled-Cluster and Møller−Plesset Perturbation Theory. *Chem. Phys. Lett.* **1998**, *290*, 423−430.
(106) Nielsen, I. M. B.; Janssen, C. L. Double-Substitution-Based Diagnostics for Coupled-Cluster and Møller−Plesset Perturbation Theory. *Chem. Phys. Lett.* **1999**, *310*, 568−576.
(107) Lee, T. J. Comparison of the T1 and D1 Diagnostics for Electronic Structure Theory: A New Definition for the Open-Shell D1 Diagnostic. *Chem. Phys. Lett.* **2003**, *372*, 362−367.
(108) Koch, H.; Jørgensen, P. Coupled Cluster Response Functions. *J. Chem. Phys.* **1990**, *93*, 3333−3344.
(109) Stanton, J. F.; Bartlett, R. J. The Equation of Motion Coupled-cluster Method. A Systematic Biorthogonal Approach to Molecular Excitation Energies, Transition Probabilities, and Excited State Properties. *J. Chem. Phys.* **1993**, *98*, 7029−7039.
(110) Geary, R. C. The Ratio of the Mean Deviation to the Standard Deviation as a Test of Normality. *Biometrika* **1935**, *27*, 310−332.
(111) Grimme, S.; Goerigk, L.; Fink, R. F. Spin-Component-Scaled Electron Correlation Methods. *Wiley Interdiscip. Rev. Comput. Mol. Sci.* **2012**, *2*, 886−906.
(112) Kozuch, S.; Gruzman, D.; Martin, J. M. L. DSD-BLYP: A General Purpose Double Hybrid Density Functional Including Spin Component Scaling and Dispersion Correction. *J. Phys. Chem. C* **2010**, *114*, 20801−20808.
(113) Hyla-Kryspin, I.; Grimme, S. Comprehensive Study of the Thermochemistry of First-Row Transition Metal Compounds by Spin Component Scaled MP2 and MP3Methods. *Organometallics* **2004**, *23*, 5581−5592.
(114) Fink, R. F. Spin-Component-Scaled Møller-Plesset (SCS-MP) Perturbation Theory: A Generalization of the MP Approach with Improved Properties. *J. Chem. Phys.* **2010**, *133*, 174113.
(115) Vydrov, O. A.; Van Voorhis, T. Nonlocal van Der Waals Density Functional: The Simpler the Better. *J. Chem. Phys.* **2010**, *133*, 244103.
(116) Perdew, J. P.; Schmidt, K. Jacob's Ladder of Density Functional Approximations for the Exchange-Correlation Energy. *AIP Conf. Proc.* **2001**, *577*, 1−20.
(117) Bistoni, G.; Riplinger, C.; Minenkov, Y.; Cavallo, L.; Auer, A. A.; Neese, F. Treating Subvalence Correlation Effects in Domain Based Pair Natural Orbital Coupled Cluster Calculations: An Out-of-the-Box Approach. *J. Chem. Theory Comput.* **2017**, *13*, 3220−3227.
(118) Najibi, A.; Goerigk, L. The Nonlocal Kernel in van Der Waals Density Functionals as an Additive Correction: An Extensive Analysis with Special Emphasis on the B97M-V and ωB97M-V Approaches. *J. Chem. Theory Comput.* **2018**, *14*, 5725−5738.

https://doi.org/10.1021/acs.jpca.1c05124
J. Phys. Chem. A 2021, 125, 8987−8999